

Cambridge University Press

978-1-107-41323-8 - Materials Issues for Tunable RF and Microwave Devices

Edited by Quanxi Jia, Felix A. Miranda, Daniel E. Oates and Xiaoxing Xi

Excerpt

[More information](#)

---

## **Frequency Agile Materials For Electronics**

Cambridge University Press

978-1-107-41323-8 - Materials Issues for Tunable RF and Microwave Devices

Edited by Quanxi Jia, Felix A, Miranda. Daniel E. Oates and Xiaoxing Xi

Excerpt

[More information](#)

---

Cambridge University Press

978-1-107-41323-8 - Materials Issues for Tunable RF and Microwave Devices

Edited by Quanxi Jia, Felix A. Miranda, Daniel E. Oates and Xiaoxing Xi

Excerpt

[More information](#)

## ANALYSIS AND OPTIMIZATION OF THIN FILM FERROELECTRIC PHASE SHIFTERS

R. R. ROMANOVSKY\*, F. W. VAN KEULS\*\*, J. D. WARNER\*, C. H. MUELLER\*, S. A. ALTEROVITZ\*, F. A. MIRANDA\*, AND A. H. QURESHI\*\*\*

\*NASA Glenn Research Center, Cleveland OH 44135

\*\*Ohio Aerospace Institute, Cleveland OH 44142

\*\*\*Cleveland State University, Cleveland OH 44101

### ABSTRACT

Microwave phase shifters have been fabricated from  $(\text{YBa}_2\text{Cu}_3\text{O}_{7-\delta}$  or  $\text{Au})/\text{SrTiO}_3$  and  $\text{Au}/\text{Ba}_x\text{Sr}_{1-x}\text{TiO}_3$  films on  $\text{LaAlO}_3$  and  $\text{MgO}$  substrates. These coupled microstrip devices rival the performance of their semiconductor counterparts at Ku- and K-band frequencies. Typical insertion loss for room temperature ferroelectric phase shifters at K-band is  $\approx 5$  dB. An experimental and theoretical investigation of these novel devices explains the role of the ferroelectric film in overall device performance. A roadmap to the development of a 3 dB insertion loss phase shifter that would enable a new type of phased array antenna is discussed.

### INTRODUCTION

Evolving high data rate communications systems demand greater attention to subtle aspects of information theory and electromagnetic engineering. As the ratio of signaling bandwidth to carrier frequency decreases, less familiar phenomena enter into system performance. And, new coding techniques are pushing channel capacity ever closer to the Shannon limit [1]. Some of these effects are expected to become quite pronounced if the trend toward wide-band scanning phased array antennas and efficient high-speed modulators continues [2]. For example, in a phased array antenna inter-element spacing, the physical size of the array, and the steering vector can conspire to introduce pulse distortion from group delay, inter-symbol interference, and beam squinting [3,4]. And the operating point of the amplifiers can affect the bit error rate depending on the modulation type and the number of carriers. Naturally one wants the phased array to operate as efficiently as possible given power limitations and thermal management problems. This desire necessitates that the power amplifiers operate in a nonlinear region near saturation. Nonlinear effects cause amplitude-to-amplitude modulation (AM/AM) and amplitude-to-phase modulation (AM/PM) distortion. The net effect of AM/AM distortion is to alternately compress and expand the signal constellation. The net effect of AM/PM conversion is a rotation of the signal constellation [3]. In a receive array, the third order intercept of the low noise amplifiers largely determines inter-modulation distortion and heat dissipation [5]. Phase shifters typically follow low noise amplifiers in a receive array and precede power amplifiers in a transmit array. Since the phase shifter's insertion loss depends on its phase setting and since its switching action represents some finite time domain response, its potential contribution to bit error rate degradation cannot generally be ignored. There will always be some effects in any phase shift keyed (PSK) modulation system, to what degree depends on the steering vector update rate and data rate.

In 1963 Berry introduced a new class of antennas that utilized an array of elementary antennas as a reflecting surface [6]. The "reflectarray" has the potential to combine the best attributes of a gimbaled parabolic reflector, low cost and high efficiency, and a direct radiating

phased array, vibration-free beam steering. A key advantage is the elimination of a complex corporate feed network. The reflectarray consists of a two-dimensional aperture characterized by a surface impedance and a primary radiator to illuminate that surface. The ferroelectric phase shifters described in this paper can be integrated with microstrip patch radiators to form a such a phase agile antenna [7]. Because the antenna elements and phase shifters can be defined using a two-step lithography process, the ferroelectric reflectarray holds promise to dramatically reduce manufacturing costs of phased array antennas and alleviates thermal management problems associated with microwave integrated circuit transmit arrays. (Note that while the devices to be described actually operate in the paraelectric regime slightly above the Curie temperature, it has become customary for workers in the field to still refer to the materials as ferroelectrics. This paper adheres to that convention.) A receive reflectarray has been designed at 19 GHz and is pictured in figure 1. The governing design assumption is a phase shifter insertion loss of 3 dB, about 40% better than we have consistently demonstrated from  $\text{Ba}_x\text{Sr}_{1-x}\text{TiO}_3$  films on  $\text{LaAlO}_3$  and  $\text{MgO}$  substrates. A circular aperture was approximated arranging 177 subarrays as shown to improve the aperture efficiency.

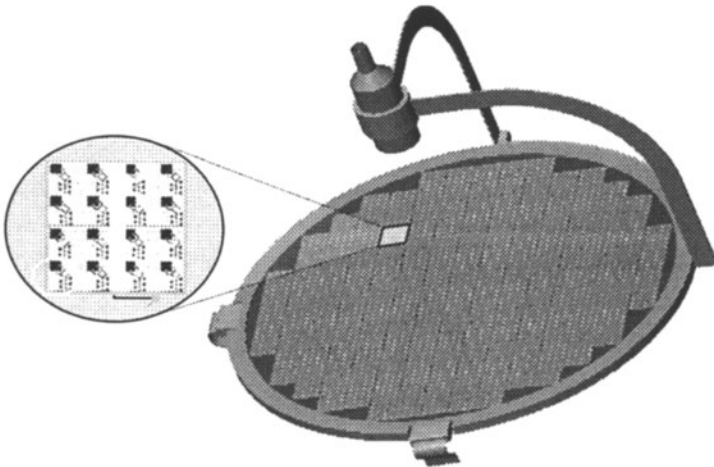


Figure 1. A 2832 element 19 GHz ferroelectric reflectarray concept. The callout shows a 16 element subarray patterned on a  $3.1 \times 3.1 \text{ cm}^2$ , 0.25 mm thick  $\text{MgO}$  substrate. The array diameter is 48.5 cm. The unit cell area is  $0.604 \text{ cm}^2$  and the estimated boresight gain is 39 dB.

The array was designed to scan past a 45 degree angle with an inter-element spacing of 0.52 wavelengths. The callout shows 16 4-section phase shifters coupled to a square patch antenna with a 90 degree hybrid coupler. The phase shifter is terminated abruptly in an open circuit and is used in a reflection mode. One output of the coupler has an additional 45° microstrip extension to feed the orthogonal edges of the patch 90° out of phase. For right hand circular polarization the phase shifter is attached to the left port of the coupler so the vertical edge of the patch receives the reflected energy with a 90° delay. While a triangular grid pattern permits the fewest elements per unit area, it was simpler to fit the phase shifters in a square unit cell. The

governing assumption in the design is that a 3 dB insertion loss phase shifter can be consistently reproduced. Indeed the phase shifter performance drives the performance and cost of the entire array. Even with a 3 dB loss device, assuming a receiver noise figure of 2 dB, the system noise temperature exceeds 800 K. Because the phase shifter is inserted between the antenna terminals and the low noise amplifier, it has the same effect as a feed line with equivalent loss in the determination of noise. The array noise does not increase with the number of elements since the noise is non-coherent but the signal at each element is correlated [8]. Assuming an aperture efficiency of 70% and a scan loss that falls off as  $\cos\theta^{1.2}$ , the gain-to-noise temperature ratio (G/T) of the array is estimated at  $\approx 3.1$  dB/K. *If the phase shifter loss could be reduced to 2 dB, the number of elements would be cut approximately in half.*

EXPERIMENT

The phase shifters analyzed here hold promise for reflectarray applications because they are compact, low-loss, and can be lithographed on the same surface as the radiating element. The designs used are based on a series of coupled microstriplines of length  $l$  interconnected with short sections of nominally  $50\ \Omega$  microstrip. The maximum coupled voltage occurs when the coupled sections are a quarter wavelength long (i.e.  $\beta l = 90^\circ$ ). Bias up to 400 V is applied to the sections via printed bias-tees consisting of a quarter-wave radial stub in series with a very high impedance quarter-wave microstrip. A sketch of the coupled microstrip cross-section is show in figure 2. By concentrating the fields in the odd mode, the phase shift per unit length is maximized and by using the ferroelectric in thin film form the effects of high loss tangent are minimized. Selecting the strip spacing “s” involves a compromise among: minimizing insertion loss, simplifying lithography, and minimizing the tuning voltage.

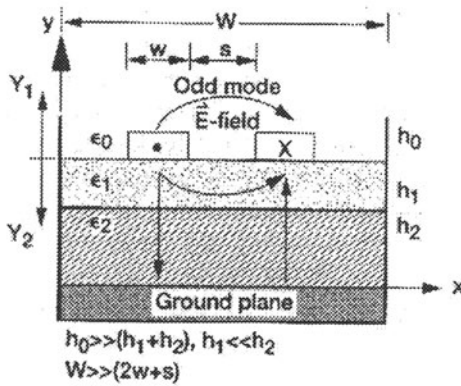


Figure 2. Cross-section of the coupled microstripline phase shifter showing the odd-mode electric field configuration.  $Y_1$  and  $Y_2$  represent the admittance looking in the positive and negative y direction, respectively, from the charge plane. The thickness of the ferroelectric layer is  $h_1$  while the host substrate has thickness  $h_2$ .

A key advantage of this technology is the relatively large feature size. Active devices at the frequencies of interest here would necessitate submicron gate length GaAs FETs. The finest feature size associated with the coupled line phase shifters is the electrode separation  $s$ , typically

Cambridge University Press

978-1-107-41323-8 - Materials Issues for Tunable RF and Microwave Devices

Edited by Quanxi Jia, Felix A. Miranda, Daniel E. Oates and Xiaoxing Xi

Excerpt

[More information](#)

$\approx 10 \mu\text{m}$ . Whereas the GaAs FET performance is largely dictated by transconductance and hence carrier transit time across the gate region, the coupled line phase shifters are static devices. The electrode gap separation determines the degree of electromagnetic coupling and the dc potential required to tune the film. As a rule-of-thumb the cutoff frequency  $f_c$  of a MESFET scales roughly with gate size as  $f_c = 9.4/l$  where the frequency is in GHz and  $l$  is in microns. Hence the ferroelectric phase shifters have much larger feature sizes at a given frequency of operation and consequently much less demanding process requirements. The total phase shift can be increased by cascading coupled line sections. Each section is linked by a 50 Ohm or so microstrip jumper. A photograph of a 4-section phase shifter patterned on 0.5 mm MgO is shown in figure 3.

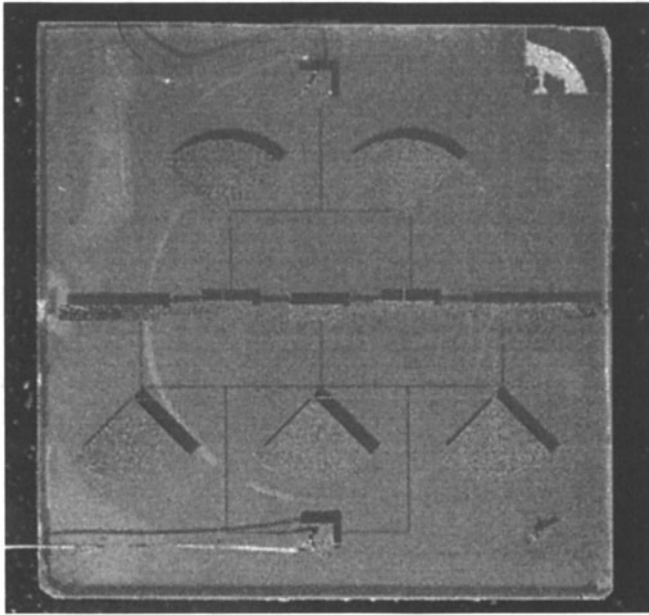


Figure 3. A 4-element  $\text{Ba}_x\text{Sr}_{1-x}\text{TiO}_3$  phase shifter on 0.5 mm MgO. The circuit measures 1 cm x 1 cm.  $l=457 \mu\text{m}$ ,  $s=10 \mu\text{m}$ , and  $w=56 \mu\text{m}$ .

These ferroelectric phase shifters are fabricated using standard lithography techniques. The “lift-off” processing recipe is straightforward. Starting with a clean substrate, AX4210 photoresist is spun on at 4000 rpm. This is followed by a soft bake at  $75^\circ\text{C}$  for 30 minutes. The photoresist is exposed through a visually translucent iron oxide mask for 30 seconds using a Carl Zeuss mask aligner with 300 nm optics. To facilitate the lift-off process, the wafer is soaked in chlorobenzene for 10 minutes at  $25^\circ\text{C}$  and blown dry with  $\text{N}_2$ . This is followed by a second bake at  $90^\circ\text{C}$  for 10 minutes. The wafer is developed for about 2 minutes in 4:1 deionized  $\text{H}_2\text{O}$ :AZ400K developer, rinsed in deionized  $\text{H}_2\text{O}$  for 5 minutes, and blown dry with  $\text{N}_2$ . Metalization consists of evaporating a 150 Angstrom adhesion layer followed by  $1.8 \mu\text{m}$  of Ag followed by a 500 Angstrom Au cap. The wafer is then soaked in acetone until the metal lifts off. It is advantageous to etch the ferroelectric from all regions except the coupled lines so that the bias tees are insensitive to tuning. A dilute 5% HF solution has been used to etch a  $\text{Ba}_x\text{Sr}_{1-x}\text{TiO}_3$

rectangular mesa beneath the coupled sections. The tradeoff is that positioning the pattern over a good region of material is tougher.

The performance of these devices is measured using an HP 8510C automatic network analyzer. The device is paced in a simple test fixture with SMA connectors and usually the launchers are attached to the microstrip input and output with silver pint. Measurements are usually done in a vacuum of about 10 mT to prevent dielectric breakdown of the air between the coupled lines. Alternatively, paraffin can be used to coat the lines but occasionally air bubbles trapped inside may contribute to arcing. In the future, a spray coated teflon coating will be used to permit safe operation under ambient conditions. Coupled microstripline FE phase shifters capitalize on the odd mode propagation constant and so have much more phase shift per unit length than simple microstripline while avoiding the need for a coplanar ground. Microwave measurements of coupled microstripline phase shifters of epitaxial  $\text{Ba}_{0.5}\text{Sr}_{0.5}\text{TiO}_3$  films grown by combustion chemical vapor deposition (CCVD) on 0.5 mm MgO showed very low loss (estimated  $\tan \delta$  was between 0.03-0.002 at 20 GHz at 23°C) [9]. As shown in figures 4 and 5, the transmission coefficient,  $S_{21}$ , at all frequencies exhibits symmetrical curve as a function of bias voltage at 297 K, as expected. The best figure of merit was 53°/dB [79]. It is evident that the hysteresis is negligible.

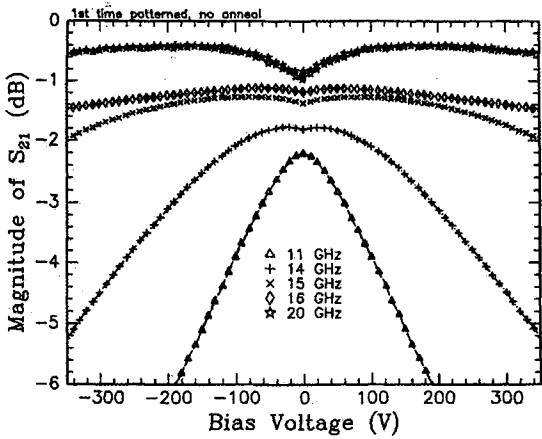


Figure 4. Measured 50  $\Omega$  4-section phase shifter on MgO at 297 K. The  $\text{Ba}_{0.50}\text{Sr}_{0.50}\text{TiO}_3$  film was grown by MicroCoating Technologies using CCVD.

The best films have been deposited by laser ablation at temperatures between 650 and 750 C and a dynamic oxygen pressure near 100 mTorr [10,11]. Thicker  $\text{Ba}_x\text{Sr}_{1-x}\text{TiO}_3$  films (>350 nm) generally exhibited poorer microwave performance despite having a clear theoretical advantage in terms of maximizing tuning as discussed in the next section. Crystalline quality unfortunately degrades as film thickness increases. The degradation is faster in  $\text{Ba}_x\text{Sr}_{1-x}\text{TiO}_3$  than in  $\text{SrTiO}_3$ .

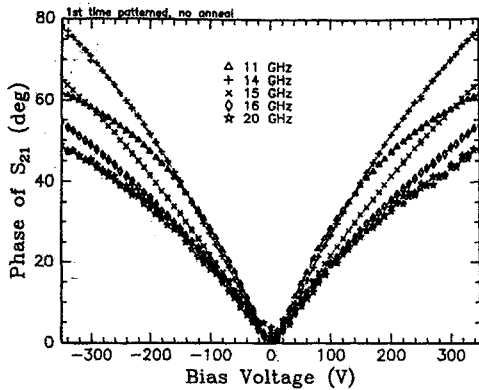


Figure 5. Measured insertion phase corresponding to figure 4.

The use of MgO ( $\epsilon_r=9.7$ ) allows wider lines for a given impedance compared to LaAlO<sub>3</sub> ( $\epsilon_r=24$ ). Consequently, the conductor loss is lower on MgO. Figures 6 and 7 show measured insertion loss and phase for 0.5  $\mu\text{m}$  Ba<sub>0.60</sub>Sr<sub>0.40</sub>TiO<sub>3</sub> film grown on 0.5 mm MgO. Choosing a operating temperature that approaches the Curie temperature from the paraelectric phase usually results in larger phase shifts but correspondingly higher loss.

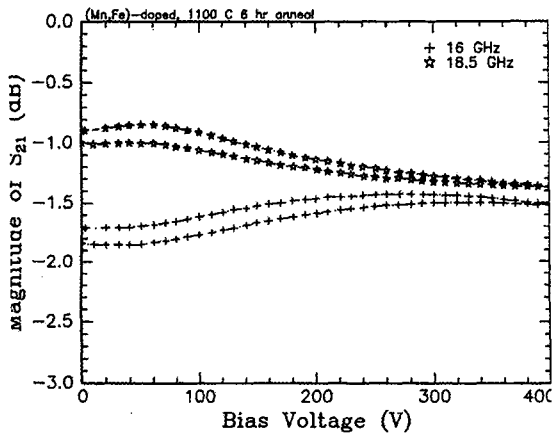


Figure 6. Measured 50 Ohm 4-element coupled line phase shifter at 210 K with Au/Cr electrodes patterned on a 0.5  $\mu\text{m}$  Ba<sub>0.60</sub>Sr<sub>0.40</sub>TiO<sub>3</sub> film grown on 0.5 mm MgO. The film was grown by the Naval Research Laboratory. These film were 1% Mn doped and annealed at 1100 C for 6 hours.

The best performance to date has been obtained from YBa<sub>2</sub>Cu<sub>3</sub>O<sub>7- $\delta$</sub>  and laser ablated SrTiO<sub>3</sub> films on (100) single crystal LaAlO<sub>3</sub> substrates [12]. Data for an 8-section nominally 50  $\Omega$  coupled microstrip device at 16 GHz is shown in figure 8. The superconducting film was 350 nm



thick and the ferroelectric film was 2.0  $\mu\text{m}$  thick. A figure of merit approaching the goal of 120  $^\circ/\text{dB}$  was obtained. It is unclear what role surface effects may have played in the superior

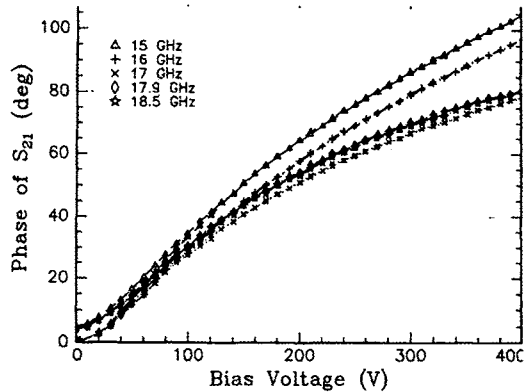


Figure 7. Measured insertion phase corresponding to figure 6.

performance of this particular phase shifter that used  $\text{YBa}_2\text{Cu}_3\text{O}_{7.8}$  electrodes instead of metal electrodes. Note that while bulk  $\text{SrTiO}_3$  is an incipient ferroelectric, thin films exhibit a relative dielectric constant maximum between 40 and 80 K.

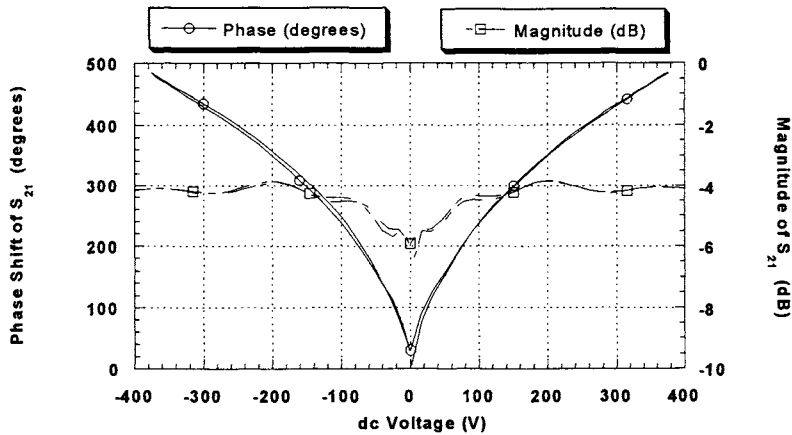


Figure 8. 8-section 50 Ohm coupled microstrip phase shifter at 40 K using  $\text{YBa}_2\text{Cu}_3\text{O}_{7.8}$  electrodes and laser ablated  $\text{SrTiO}_3$  films on (100) single crystal 0.25 mm  $\text{LaAlO}_3$ . Hysteresis is unremarkable.  $l=470\text{ }\mu\text{m}$ ,  $s=7.5\text{ }\mu\text{m}$ , and  $w=25\text{ }\mu\text{m}$ .

Some recent results suggest that after extended voltage cycling an anomalous discontinuity in loss and phase occurs under certain bias and film growth conditions. The origin of this polarization change is not understood at this time. Fatiguing effects have been observed in ferroelectric films for DRAM applications, where occasionally micro-cracks occur to absorb the stress. Such effects are irreversible. The study of this phenomenon is ongoing.

DEVICE MODELING

The multi-layer structure has been analyzed using a computationally efficient variational method to calculate the even and odd mode capacitance [7,13]. If a quasi-TEM type of propagation is assumed the propagation constant and impedance can be completely determined from line capacitance. Since the cascaded coupled line circuit resembles a series of one-pole bandpass filters, as the dc bias increases, the dielectric constant of the BST film decreases, causing the passband to rise in frequency and the  $\tan \delta$  of the BST to decrease. The impedance matrix of the cascaded network can be derived by well-known coupled line theory using the superposition of even and odd mode excitation. Then an equivalent S-parameter model can be extracted and used to predict the pass-band characteristics of the phase shifter.

The bandwidth compression from tuning is evident in figure 9 which is data from an 8-section phase shifter on 0.3 mm MgO using a 400 nm  $\text{Ba}_{0.60}\text{Sr}_{0.40}\text{TiO}_3$  laser ablated film. The roll-off at the upper end of the frequency range is attributed to bias-tee effects.

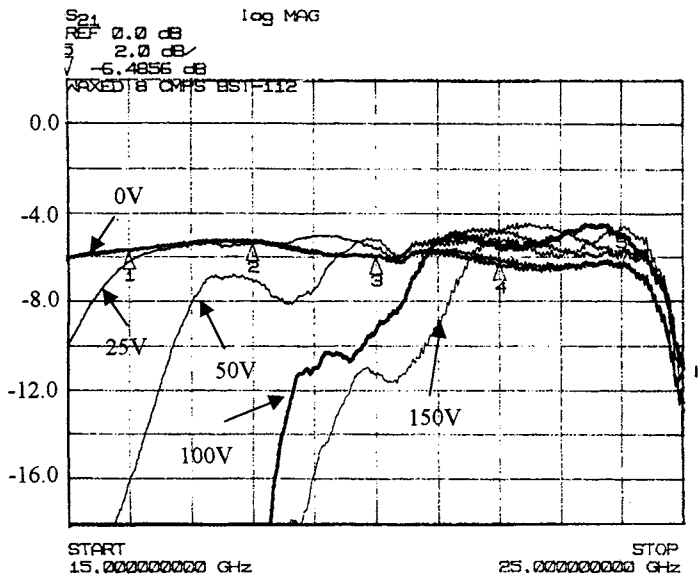


Figure 9. Measured Insertion Loss (including SMA launchers) of an 8-element  $\approx 50 \, \Omega$  PLD coupled microstripline phase shifter at 290 K as a function of bias voltage. Substrate is 0.3 mm MgO with 400 nm  $\text{Ba}_{0.60}\text{Sr}_{0.40}\text{TiO}_3$  film.  $l=350 \, \mu\text{m}$ ,  $s=7.5 \, \mu\text{m}$  and  $w=30 \, \mu\text{m}$ . Bandwidth compression from the filtering effect is evident. Marker 1, 2, 3, and 4 are at  $-5.75$ ,  $-5.38$ ,  $-6.00$ , and  $-6.49$  dB, respectively.

In order to gauge the impact of the ferroelectric film on overall performance, Table 1 summarizes several important parameters for a *single* coupled microstrip section on  $h_2=0.3$  mm MgO ( $\epsilon=9.7$ ) derived using the quasi-TEM analysis where  $\epsilon_1$  and  $h_1$  correspond to figure 2. The